Applied Physics Letters

Piezotronic effect on Rashba spin–orbit coupling based on $MAPbI_3$/ZnO heterostructures

Cite as: Appl. Phys. Lett. **117**, 071601 (2020); https://doi.org/10.1063/5.0011280
Submitted: 21 April 2020 . Accepted: 31 July 2020 . Published Online: 18 August 2020

Laipan Zhu, and Zhong Lin Wang

Lock-in Amplifiers
up to 600 MHz

© 2020 Author(s).

Applied Physics Letters ARTICLE scitation.org/journal/apl

Piezotronic effect on Rashba spin–orbit coupling based on $MAPbI_3$/ZnO heterostructures

Cite as: Appl. Phys. Lett. **117**, 071601 (2020); doi: 10.1063/5.0011280
Submitted: 21 April 2020 · Accepted: 31 July 2020 ·
Published Online: 18 August 2020

View Online

Export Citation

CrossMark

Laipan Zhu[1,2] and Zhong Lin Wang[1,2,3,a)]

AFFILIATIONS

[1]CAS Center for Excellence in Nanoscience, Beijing Key Laboratory of Micro-Nano Energy and Sensor, Beijing Institute of Nanoenergy and Nanosystems, Chinese Academy of Sciences, Beijing 100083, People's Republic of China
[2]School of Nanoscience and Technology, University of Chinese Academy of Sciences, Beijing 100049, People's Republic of China
[3]School of Material Science and Engineering, Georgia Institute of Technology, Atlanta, Georgia 30332, USA

[a)]Author to whom correspondence should be addressed: zhong.wang@mse.gatech.edu

ABSTRACT

Rashba spin–orbit coupling (SOC) is a core issue in semiconductor spintronics, which allows the manipulation of electron spin through an electric field rather than an external magnetic field, revealing a bright prospect for advanced electronic devices with ultra-high speed and integration. Conversely, the emerging piezotronic effect is the born characteristic for many semiconductors that have a non-central symmetric structure, such as ZnO and GaN. Here, we design three heterostructure devices, based on piezoelectric p-type $(CH_3NH_3)PbI_3$ single crystals and n-type wurtzite-structured ZnO thin films, to theoretically study how the piezotronic effect can effectively work on the Rashba spin–orbit coupling. Benefiting from large piezoelectric charges at the interface when a vertical strain is applied, a high concentration of two-dimensional electron gas is induced in the plane of the heterostructure, which can tune the built-in electric field at the interface and further manipulate the Rashba SOC. With the increase in pressure, both the Rashba parameter and spin splitting are found to first vanish and then increase linearly for ZnO with doping densities of 10^{15} and 10^{16} cm^{-3}. This work provides insight for manipulating electron spins via the introduction of piezocharges, showing great application potential of the piezotronic effect in tuning spintronic devices.

Published under license by AIP Publishing. https://doi.org/10.1063/5.0011280

Semiconductor spintronics is developing rapidly due to its bright prospect in advanced electronic devices with ultra-high speed, ultra-high integration, and ultra-low power consumption.[1,2] Spin–orbit coupling (SOC) is an important and effective way to tune the spin splitting and spin transport by the introduction of space inversion asymmetry. In quantum wells or heterostructures, the SOC is believed to derive from the Dresselhaus term caused by bulk inversion asymmetry (BIA) and the Rashba term resulted from structure inversion asymmetry (SIA), which can be controlled by applying an external electric field.[3–5] The SOC can be regarded as a $\boldsymbol{k}$-dependent effective magnetic field, which causes a spin procession when carriers are transported in a semiconductor. The efficient control of Rashba SOC and its corresponding spin transport via external fields is the core issue in realizing high-performance semiconductor spin devices.

In recent years, the piezotronic and piezophototronic effects have been attracting much attention in improving the performance of electronic and optoelectronic devices. These two emerging effects are born characteristics in semiconductor-piezoelectric materials that lack central symmetry, such as third-generation wurtzite semiconductors (ZnO, GaN, CdS, etc.), transition-metal dichalcogenides (MoS_2, WSe_2, etc.), and perovkites.[6–8] So far, they have been widely applied in micro-nanodevices, such as transistors,[9,10] diodes,[11] solar cells,[12,13] light emission diodes,[14,15] and photodetectors.[16,17] Recently, we have demonstrated experimentally that the piezopotential, regarded as a "gate" voltage, can be used to effectively tune the Rashba SOC in both P3HT/ZnO nanowire heterostructures and cation-mixed perovskite nanowires.[18,19] Compared to the piezopotential, the piezoelectric charges (abbreviated as piezocharges) at the interfaces or heterostructures can not only tune the SIA or interface electric field as what the piezopotential does but also induce an in-plane two-dimensional electron gas (2DEG), which may make this kind of manipulation much more efficient due to the confined spin-polarized electrons in the triangular quantum wells. If a circularly polarized light is applied to irradiate on the heterointerface, the transportation of photoinduced spin-polarized electrons in the triangular quantum wells can be further tuned by the Rashba SOC. However, the study of the detailed influence of piezocharges on Rashba SOC or spin transport has been rarely reported.

Published under license by AIP Publishing

In this work, we study theoretically on how the piezocharges affect the Rashba SOC from a quantitative perspective. Here, organic–inorganic $(CH_3NH_3)PbI_3$ (abbreviated as $MAPbI_3$) is selected as the candidate of p-type material due to the fact that its single-crystal structure possesses a big piezoelectric coefficient. An n-type ZnO thin film with a wurtzite structure is used in view of its simple form of Dresselhaus SOC as well as its good piezoelectric property. The large number of positive piezocharges can attract vast free electrons at the interface of ZnO, forming a high concentration of 2DEG, which can tune the built-in electric field at the interface and further manipulate the Rashba SOC.

From Fig. 1(a), one can see that the *c*-axis directions in the two semiconductor materials are intentionally reversed and point away from the interface. To simplify the calculation, we neglect the lattice mismatch of $MAPbI_3$ and ZnO. When no stress is applied on the devices, there will be space charge regions with positive charges at the ZnO side and negative charges at the $MAPbI_3$ side. The built-in electric potential energy of the n-ZnO/p-$MAPbI_3$ heterojunction can be calculated as $eV_D = E_{Fn}(\mathrm{ZnO}) - E_{Fp}(\mathrm{MAPbI_3})$, where e is the electron charge, V_D is the built-in electric potential, E_F is the Fermi energy. If the electron density is set to 10^{17}, 10^{16}, and $10^{15}\,\mathrm{cm^{-3}}$, the Fermi energy E_F is calculated to be -4.44, -4.5, and -4.56 eV (see the supplementary material for the detailed calculation). For solution-grown single crystal $MAPbI_3$, a weak p-doped property with a low free hole concentration of $\sim 10^{10}\,\mathrm{cm^{-3}}$ had been revealed.[20] Here, the Fermi energy E_F of single crystal $MAPbI_3$ was adopted to be -4.8 eV.[20,21] Then, a schematic diagram of the energy band of the heterostructure can be plotted, as shown in Fig. 1(b). The inner built-in electric field in ZnO and $MAPbI_3$ can be expressed as

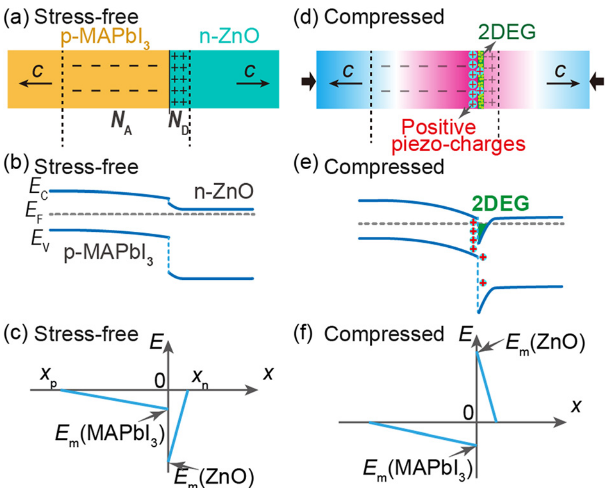

FIG. 1. (a) Schematic diagram of the space charge zone at the interface of p-$MAPbI_3$/n-ZnO. (b) The contact band diagram of the p-$MAPbI_3$/n-ZnO junction without applying compressive pressure. (c) Schematic distribution of the inner electric field in the p–n junction. (d) Energy band diagram when a compressive pressure is applied, denoting the distribution of piezopotential, positive piezocharges, and 2DEG. (e) The band diagram of the p–n junction when applying a compressive pressure. (f) Schematic distribution of the inner electric field in the p–n junction when applying a compressive pressure.

$$E(x) = \frac{qN_D(x - x_n)}{\varepsilon_r(\mathrm{ZnO})\varepsilon_0}, \quad (0 < x < x_n), \tag{1}$$

$$E(x) = -\frac{qN_A(x - x_p)}{\varepsilon_r(\mathrm{MAPbI_3})\varepsilon_0}, \quad (-x_p < x < 0), \tag{2}$$

where ε_r, ε_0, x_n, and x_p are the relative permittivity, the vacuum permittivity, the width of the space charge region in ZnO, and the width of the space charge region in $MAPbI_3$, respectively. For the n^+p junction, one can get $x_p \gg x_n$, and the width of the total space charge region X_D is approximately equal to that in $MAPbI_3$, that is, $X_D \approx x_p$. x_p can be expressed as

$$x_p = \sqrt{\frac{2\varepsilon_r(\mathrm{MAPbI_3})\varepsilon_0 V_D}{qN_A}}, \tag{3}$$

where $V_D = [E_F(\mathrm{ZnO}) - E_F(\mathrm{MAPbI_3})]/e = 0.36$, 0.3, and 0.24 V for electron densities of 10^{17}, 10^{16}, and $10^{15}\,\mathrm{cm^{-3}}$, respectively. Using $\varepsilon_r(\mathrm{MAPbI_3}) = 9$, one can get x_p = 357, 325, and 291 μm for electron densities of 10^{17}, 10^{16}, and $10^{15}\,\mathrm{cm^{-3}}$, respectively. According to $x_n = N_A x_p / N_D$, x_n can be obtained to be 0.035, 0.325, and 2.91 nm for electron densities of 10^{17}, 10^{16}, and $10^{15}\,\mathrm{cm^{-3}}$, respectively, and hence, they are abrupt heterojunctions especially for the case of $10^{17}\,\mathrm{cm^{-3}}$. The initial maximum values of built-in electric fields E_0 in ZnO (at the interface of $MAPbI_3$/ZnO, i.e., $x = 0$) are calculated to be -70, -65, and -58 V/cm, and Fig. 1(c) shows a schematic distribution of the inner electric field in the p–n^+ junction.

When a vertical pressure is applied on the devices, there will be positive piezocharges induced at the interface, as shown in Fig. 1(d). The piezocharge density can be expressed as

$$p_{\mathrm{piezo}} = d_{33}\sigma_z, \tag{4}$$

where d_{33} and σ_z are the piezoelectric coefficient and the pressure applied along the *z*-axis, respectively. For the ZnO thin film and $MAPbI_3$ single crystal, d_{33} are experimentally measured to be 11.4 pC/N and 31.4 pC/N from the former literature, respectively.[22,23] The effective piezocharge density at the interface of ZnO/$MAPbI_3$ is the sum of positive piezocharge densities of ZnO and $MAPbI_3$, namely, $p_{\mathrm{piezo}} = [d_{33}(\mathrm{ZnO}) + d_{33}(\mathrm{MAPbI_3})]\sigma_z = d_{33}^*\sigma_z$, where d_{33}^* is the effective piezoelectric coefficient and the units of p_{piezo} and σ_z are $\mathrm{nC/m^2}$ and kPa, respectively. Here, the screening effect for piezocharges due to free carriers in bulk ZnO and $MAPbI_3$ is the driving force of forming 2DEG. The calculated piezocharge density as a function of pressure is shown in Fig. 2(a).

If a compressive pressure of 1 MPa is applied on the device (an ideal state), one can estimate that a large positive piezocharge density

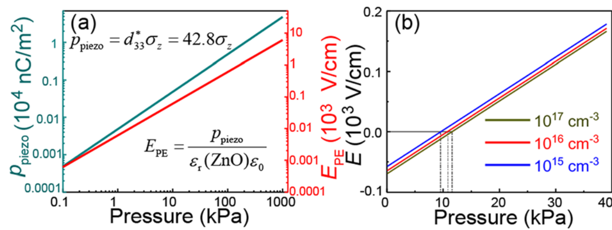

FIG. 2. (a) Piezocharge density and piezoelectric field as a function of vertical pressure. (b) Effective electric field as a function of vertical pressure when different doping densities in ZnO are adopted.

Published under license by AIP Publishing

of 42.8 μC/m^2 can be induced at the interface. Hence, electrons in ZnO will be attracted to screen the positive piezocharges. Supposing that all the whole positive piezocharges are screened by electrons attracted from ZnO, there will be a large 2DEG at the heterointerface [see Figs. 1(e) and 1(f)] with the electron density of 42.8 μC/m^2, which will elicit an equivalent piezoelectric field $E_{\rm PE}$ of 5.4×10^3 V/cm by using the following equation:

$$E_{\rm PE}=\frac{p_{\rm piezo}}{\varepsilon_{\rm r}({\rm ZnO})\varepsilon_0}, \tag{5}$$

where $\varepsilon_{\rm r}$(ZnO) = 9 is adopted [see Fig. 2(a)]. This piezoelectric field is about two orders of magnitude larger than that of the built-in electric field, revealing good potential in tuning the interface electric field. For simplicity and considering the ultra-thin width of 2DEG, the 2DEG in ZnO is supposed to locate at $x=0$ with the maximum inner electric field. As the direction of the piezoelectric field is opposite to that of the inner electric field without applying pressure, a vertical pressure of about 10 kPa is enough to make the total effective electric field zero, and the needed pressure is a little bit larger for higher doped ZnO [see Fig. 2(b)]. The effective electric field will reverse the sign to positive if the pressure is further increased, as shown in Figs. 1(f) and 2(b).

The Hamiltonian of SOC can be written in the form

$$H_{\rm SO}=\boldsymbol{\sigma}\cdot\boldsymbol{B}_{\rm eff}(\boldsymbol{k}), \tag{6}$$

where $\boldsymbol{B}_{\rm eff}(\boldsymbol{k})$ is an effective magnetic field, which is not a real magnetic field, and hence, it cannot break the time-reversal symmetry.[24,25] The wurtzite semiconductors with the C_{6v} point group are gyrotropic, which allows a $\boldsymbol{k}$-linear spin splitting.[25] Considering that the electrons in quantum wells are distributed near the Γ point in the momentum space, the SOC term of 2DEG in wurtzite ZnO grown along [0001] and with the lattice symmetry of C_{6v} can be expressed as[25–28]

$$H_{\rm SO}=(\alpha+\beta)(\boldsymbol{\sigma}\times\boldsymbol{k})_z=(\alpha+\beta)\left(\sigma_x k_y-\sigma_y {\rm k}_x\right), \tag{7}$$

where k, α, β, and σ are the electron momentum, the Rashba parameter, the Dresselhaus parameter, and Pauli matrix, respectively. It is to be noted that BIA also results in a $\boldsymbol{k}$-linear spin splitting near the Γ point due to the energy quantization in the k_z direction, whose form is strictly the same as that of [111]-grown zinc blende quantum wells or 2DEG.[25,28] α is in direct proportion to the interface electric field E through the linear relation

$$\alpha=e\alpha_0 E=e\alpha_0(E_{\rm PE}+E_0), \tag{8}$$

where α_0 is the so-called Rashba coefficient related to the band structure.[29] From the $\mathbf{k}\cdot\mathbf{p}$ theory, α_0 for the asymmetric heterostructure is estimated to be proportional to the spin–orbit splitting energy $\Delta_{\rm so}$ while inversely proportional to the square of the bandgap.[30,31] The value of $\Delta_{\rm so}$ for the ZnO 2DEG is unclear. However, the Rashba parameter in ZnO bulk has been calculated to be 1.1 meV Å. We suppose the Rashba value in this ZnO 2DEG to be 1.1 meV Å when no strain is applied on the heterostructure, but actually it should be larger than this value. Then, the Rashba coefficients are estimated to be $\alpha_0=1.57\times10^3$, 1.69×10^3, and 1.9×10^3 Å^2 for ZnO electron densities of 10^{17}, 10^{16}, and 10^{15} cm^{-3}, respectively. The pressure dependence of Rashba parameters is calculated, as shown in Fig. 3(a). It can be seen that the Rashba parameters for the three samples are all increased linearly with the increase in vertical pressure, and the value

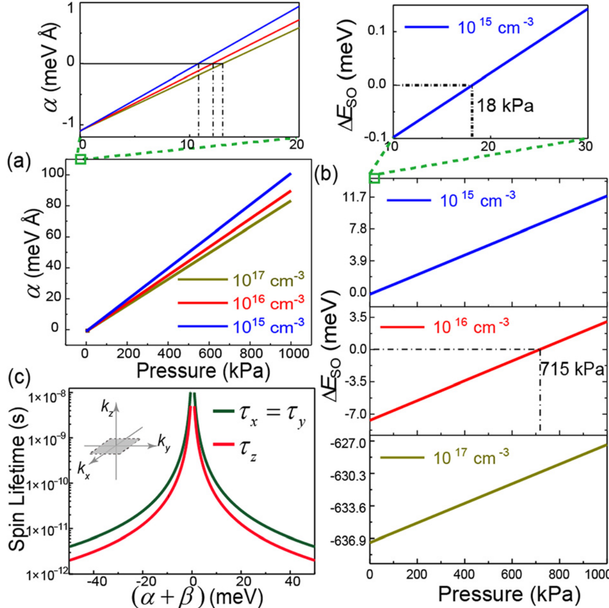

FIG. 3. (a) Pressure dependence of the Rashba parameter for different doping densities of ZnO. The upper inset shows an enlarged zone for smaller pressure. (b) Pressure dependence of spin splitting of the conduction band for different doping densities of ZnO, and the upper inset shows an enlarged view for pressure ranging from 10 to 30 kPa in the case of 10^{15} cm^{-3}. (c) Spin lifetime as a function of total SOC parameter.

of the total Rashba parameter can be wiped out under pressures of 13, 12.1, and 10.8 kPa for ZnO electron densities of 10^{17}, 10^{16}, and 10^{15} cm^{-3}, respectively. In other words, it needs more pressure to offset the stronger initial inner electric field in heavily doped ZnO. The total spin splitting of the energy band resulting from the spin–orbit interaction can be expressed as

$$\Delta E_{\rm SO}=2k\left[(e\alpha_0 E_0+\beta)+\frac{e\alpha_0 d_{33}^*}{\varepsilon_r\varepsilon_0}\sigma_z\right]. \tag{9}$$

The Rashba and Dresselhaus terms in 2DEG based on wurtzite-type semiconductors can be designed to have opposite signs.[25,27] In the calculation, it is assumed that $\alpha>0$ and $\beta<0$ after the 2DEG is formed and that $\alpha<0$ and $\beta<0$ before the 2DEG is formed. This assumption may affect the value of the effective piezoelectric coefficient, but the main conclusions of the pressure dependence of SOC should be the same. According to the former calculation of this paper, the widths of the triangular quantum well in the z direction are 0.035, 0.325, and 2.91 nm for electron densities of 10^{17}, 10^{16}, and 10^{15} cm^{-3}, respectively. According to the uncertainty principle, $\Delta z\cdot\Delta k_z\geq 1/2$, and considering that the half maximum of the wave function in the z direction is a bit smaller than the width of the triangular quantum well, we suppose $\Delta z\cdot\Delta k_z=1/\sqrt{2}$. Then, one can estimate $k_z\approx\Delta k_z$ to be 2, 0.22, and 0.024 Å^{-1}. Hence, the Dresselhaus coefficients β are estimated to be −5400, −64, and −0.75 meV Å for electron densities of 10^{17}, 10^{16}, and 10^{15} cm^{-3}, respectively, by using $\beta=\gamma b k_z^2$,[27] where $\gamma=0.33$ eV Å^3 and $b\approx4$. The pressure dependences of the total spin splitting around the Γ point, here using $k=0.03(2\pi/a)$, of the

Published under license by AIP Publishing

conduction band are calculated (where $a = 3.25$ Å is the in-plane lattice constant of ZnO), as shown in Fig. 3(b). The spin splitting for ZnO with an electron density of $10^{17}\,\text{cm}^{-3}$ is relatively large due to the huge Dresselhaus SOC, and hence, the manipulation of the total SOC by pressure is inefficient. But for ZnO with an electron density of $10^{16}\,\text{cm}^{-3}$, a pressure of 715 kPa can make the spin splitting zero. A much smaller pressure of 18 kPa is enough to wipe out the spin splitting for ZnO with an electron density of $10^{15}\,\text{cm}^{-3}$. As [0001]-grown wurtzite 2DEGs hold the same configuration as [111]-grown zinc blende quantum wells or 2DEGs, the electron spin lifetime for ZnO is believed to obey the following expression:[32]

$$\tau_x = \tau_y = 2\tau_z \propto (\alpha + \beta)^{-2}. \quad (10)$$

As shown in Fig. 3(c), the spin lifetime increases tremendously when the total SOC or spin splitting is gradually vanished, and the manipulation of Rashba SOC by applying pressure can effectively tune the spin lifetime.

The in-plane effective magnetic field resulting from the spin–orbit interaction can be expressed as

$$\boldsymbol{B}_{\text{eff}} = \left[(e\alpha_0 E_0 + \beta) + \frac{e\alpha_0 d_{33}^*}{\varepsilon_r \varepsilon_0} \sigma_z \right] (k_y, -k_x). \quad (11)$$

When the direction of electron spin is parallel to the direction of the effective magnetic field, the energy band of electrons with a parallel (or antiparallel) spin direction will split with an increased (or a reduced) energy of $\Delta E_{SO}/2$. $\boldsymbol{B}_{\text{eff}}$ is anticlockwise without applying pressure. The directions of spin-up and spin-down correspond to the directions parallel and antiparallel to $\boldsymbol{B}_{\text{eff}}$, respectively,. With the increase in pressure, $\boldsymbol{B}_{\text{eff}}$ will be reduced to zero and then increased clockwise in the k_x–k_y plane; meanwhile, the spin splitting will also be reduced to zero first and then become stronger (see supplementary material Fig. S1). For strong SOC enhanced by pressure, one can use optical methods, such as the circular photogalvanic effect (CPGE) measurement, to realize an efficient spin injection;[3,26,33] and a pressure-gated spin field-effect transistor can also be achieved when the effective magnetic field works in ON and OFF states (see supplementary material Fig. S2).[34]

In conclusion, a piezoelectric p-MAPbI_3/n-ZnO heterostructure is studied theoretically. Applying vertical pressure can induce a large number of positive piezocharges, which will attract vast electrons at the interface of ZnO, forming a high concentration of 2DEG. The 2DEG can tune the built-in electric field at the interface and further manipulate the Rashba SOC. With the increase in pressure, the effective electric field, the Rashba parameter, and the spin splitting are all vanished first and then increased linearly for ZnO with doping densities of 10^{15} and $10^{16}\,\text{cm}^{-3}$. Proper pressures of 18 and 715 kPa for ZnO with doping densities of 10^{15} and $10^{16}\,\text{cm}^{-3}$ are discovered, respectively, to make the total spin splitting disappear, resulting in a much longer electron spin relaxation time. The materials selection for this piezotronic effect enhanced SOC should be the p–n junction including at least one piezoelectric semiconductor, and the p–n junction should also form a quantum well or 2DEG. The calculation is an ideal case, which may be different with the actual measurement because the pressure endurance of the materials and possible interface states, etc., are not taken into consideration. However, this work provides insight for manipulating electron spins via the introduction of piezocharges, opening up another cross-cutting research field by combining piezotronics with semiconductor spintronics.

See the supplementary material for the calculation of Fermi energy of ZnO, the schematic diagrams of the pressure dependence of the effective magnetic field and spin splitting, and the two application scenarios for pressure-controlled spin injectors and spin field transistors.

This research was supported by the National Natural Science Foundation of China (Grant Nos. 11704032, 51432005, 5151101243, and 51561145021), the National Key R&D Project from Minister of Science and Technology (No. 2016YFA0202704), and the Beijing Municipal Science and Technology Commission (Nos. Z171100000317001, Z171100002017017, and Y3993113DF).

DATA AVAILABILITY

The data that support the findings of this study are available within this article and its supplementary material.

REFERENCES

[1] D. D. Awschalom and M. E. Flatte, Nat. Phys. **3**, 153 (2007).
[2] A. Manchon, H. C. Koo, J. Nitta, S. M. Frolov, and R. A. Duine, Nat. Mater. **14**, 871 (2015).
[3] S. Ganichev and W. Prettl, J. Phys. **15**, R935 (2003).
[4] G. Dresselhaus, Phys. Rep. **100**, 580 (1955).
[5] E. I. Rashba, Sov. Phys., Solid State **2**, 1109 (1960).
[6] Z. L. Wang, Adv. Mater. **24**, 4632 (2012).
[7] Z. L. Wang, Nano Today **5**, 540 (2010).
[8] Z. L. Wang, Mater. Today **10**, 20 (2007).
[9] L. Wang, S. Liu, G. Gao, Y. Pang, X. Yin, X. Feng, L. Zhu, Y. Bai, L. Chen, T. Xiao, X. Wang, Y. Qin, and Z. L. Wang, ACS Nano **12**, 4903 (2018).
[10] W. Wu, X. Wen, and Z. L. Wang, Science **340**, 952 (2013).
[11] J. Zhou, P. Fei, Y. Gu, W. Mai, Y. Gao, R. Yang, G. Bao, and Z. L. Wang, Nano Lett. **8**, 3973 (2008).
[12] L. Zhu and Z. L. Wang, Adv. Funct. Mater. **29**, 1808214 (2019).
[13] L. Zhu, L. Wang, F. Xue, L. Chen, J. Fu, X. Feng, T. Li, and Z. L. Wang, Adv. Sci. **4**, 1600185 (2017).
[14] M. Chen, C. Pan, T. Zhang, X. Li, R. Liang, and Z. L. Wang, ACS Nano **10**, 6074 (2016).
[15] X. Li, M. Chen, R. Yu, T. Zhang, D. Song, R. Liang, Q. Zhang, S. Cheng, L. Dong, A. Pan, L. Wang Zhong, J. Zhu, and C. Pan, Adv. Mater. **27**, 4447 (2015).
[16] P. Lin, L. Zhu, D. Li, L. Xu, C. Pan, and Z. Wang, Adv. Funct. Mater. **28**, 1802849 (2018).
[17] Q. Lai, L. Zhu, Y. Pang, L. Xu, J. Chen, Z. Ren, J. Luo, L. Wang, L. Chen, K. Han, P. Lin, D. Li, S. Lin, B. Chen, C. Pan, and Z. L. Wang, ACS Nano **12**, 10501 (2018).
[18] L. Zhu, Y. Zhang, P. Lin, Y. Wang, L. Yang, L. Chen, L. Wang, B. Chen, and Z. L. Wang, ACS Nano **12**, 1811 (2018).
[19] L. Zhu, Q. Lai, W. Zhai, B. Chen, and Z. L. Wang, Mater. Today **37**, 56 (2020).
[20] Q. Dong, Y. Fang, Y. Shao, P. Mulligan, J. Qiu, L. Cao, and J. Huang, Science **347**, 967 (2015).
[21] P. Cui, D. Wei, J. Ji, H. Huang, E. Jia, S. Dou, T. Wang, W. Wang, and M. Li, Nat. Energy **4**, 150 (2019).
[22] X. B. Wang, C. Song, D. M. Li, K. W. Geng, F. Zeng, and F. Pan, Appl. Surf. Sci. **253**, 1639 (2006).
[23] S. Liu, F. Zheng, I. Grinberg, and A. M. Rappe, J. Phys. Chem. Lett. **7**, 1460 (2016).
[24] P. S. Eldridge, W. J. H. Leyland, P. G. Lagoudakis, O. Z. Karimov, M. Henini, D. Taylor, R. T. Phillips, and R. T. Harley, Phys. Rev. B **77**, 125344 (2008).

Published under license by AIP Publishing

[25]S. D. Ganichev and L. E. Golub, Phys. Status Solidi B **251**, 1801 (2014).
[26]C. Yin, B. Shen, Q. Zhang, F. Xu, N. Tang, L. Cen, X. Wang, Y. Chen, and J. Yu, Appl. Phys. Lett. **97**, 181904 (2010).
[27]J. Y. Fu and M. W. Wu, J. Appl. Phys. **104**, 093712 (2008).
[28]R. Eppenga and M. F. H. Schuurmans, Phys. Rev. B **37**, 10923 (1988).
[29]M. A. Leontiadou, K. L. Litvinenko, A. M. Gilbertson, C. R. Pidgeon, W. R. Branford, L. F. Cohen, M. Fearn, T. Ashley, M. T. Emeny, B. N. Murdin, and S. K. Clowes, J. Phys. **23**, 035801 (2011).
[30]E. A. de Andrada e Silva, G. C. La Rocca, and F. Bassani, Phys. Rev. B **50**, 8523 (1994).
[31]F. G. Pikus and G. E. Pikus, Phys. Rev. B **51**, 16928 (1995).
[32]X. Cartoixà, D. Z. Y. Ting, and Y. C. Chang, Phys. Rev. B **71**, 045313 (2005).
[33]Q. Zhang, X. Wang, C. Yin, F. Xu, N. Tang, B. Shen, Y. Chen, K. Chang, W. Ge, and Y. Ishitani, Appl. Phys. Lett. **97**, 041907 (2010).
[34]I. Žutić, J. Fabian, and S. Das Sarma, Rev. Mod. Phys. **76**, 323 (2004).

Published under license by AIP Publishing